IJMCM
International Journal of Molecular and Cellular Medicine
p-ISSN: 2251-9637 o-ISSN: 2251-9645
Babol University of Medical Sciences
Cellular and Molecular Biology Research Center

# Astaxanthin Co-treatment with Low Dose Methotrexate Increases the Cell Cycle Arrest and Ameliorates the Methotrexate-induced Inflammatory Response in NALM-6

**Nastaran Moridi[1], Mahsa Najafzadeh[1], Mahtab Sayedi[2*], Seyed Mehdi Sajjadi[2*]**

*1. Student Research Committee, Birjand University of Medical Sciences, Birjand, Iran.*
*2. Cellular and Molecular Research Center, Birjand University of Medical Sciences, Birjand, Iran.*

**Article type:**
**Original Article**

**Received:**
2024.01.28
**Revised:**
2024.07.02
**Accepted:**
2024.07.07

**ABSTRACT**

Methotrexate (MTX), an antimetabolite agent, is widely used for acute lymphoblastic leukemia treatment, despite its association with significant organ dysfunction. Astaxanthin (AST) is a natural carotenoid which has recently been emerged as a promising anti-tumor and anti-inflammatory agent. In this study, we aimed to evaluate the effectiveness of astaxanthin and low-dose methotrexate co-treatment in acute lymphoblastic leukemia cell line. The expression of Dihydrofolate reductase (DHFR), Thymidylate synthase (TYMS), apoptotic, anti-apoptotic as well as inflammatory genes was investigated using qRT-PCR. Flow cytometry was performed for cell cycle quantitative evaluation. Clonogenic assay was used to assess NALM6 cells proliferation capacity following treatment with AST, MTX, and co-treatment. To compare the antioxidant property of each group, the ferric ion reducing anti-oxidant power assay was performed. A reduction in viability was observed in the presence of MTX, AST, and their combined treatment. Both AST alone and in combination with MTX caused cell cycle arrest and a reduction in the expression of DHFR and TYMS. While MTX, AST, and their combination could reduce STAT3 and BCL-XL gene expression, they could act as positive regulators for the expression of BAX and CASP3, TNFα, and IL6. AST and MTX co-treatment inhibited the colony formation ability. FRAP assay also revealed that AST and AST+MTX increased the antioxidant capacity. Our data suggests that AST can improve MTX treatment efficacy and their combination therapy can be considered as a promising strategy for the management of acute lymphoblastic leukemia.

**Keywords:** Acute lymphoblastic leukemia, Astaxanthin, Methotrexate, NALM-6

**Cite this article**: Moridi N, *et al*. Astaxanthin Co-treatment with Low Dose Methotrexate Increases the Cell Cycle Arrest and Ameliorates the Methotrexate-induced Inflammatory Response in NALM-6. *International Journal of Molecular and Cellular Medicine*. 2024; 13(2):133-146. **DOI:** 10.22088/IJMCM.BUMS.13.2.133

*Corresponding 1: Mahtab Sayadi
Address: Cellular and Molecular Research Center, Birjand University of Medical Sciences, Birjand, Iran.
E-mail: sayadi.mahtab@yahoo.com
*Corresponding 2: Seyed Mehdi Sajjadi
Address: Cellular and Molecular Research Center, Birjand University of Medical Sciences, Birjand, Iran.
E-mail: mehdi.sadjadi@bums.ac.ir

## Introduction

Acute lymphoblastic leukemia (ALL), a hematologic disorder, is characterized by abnormal development, growth, and buildup of lymphoid progenitor cells in the bone marrow or extra-medullary areas (1). Although childhood ALL shows an encouraging prognosis with 80–90% survivability, adult ALL treatment is more challenging and unfortunately only 20-40% of patients can recover (2). However, recent implementation of novel treatment approaches has improved survival rate of these individuals (3).

Methotrexate (MTX), widely recognized chemotherapy medication, inhibits DNA synthesis by the inhibition of various enzymes including dihydrofolate reductase (DHFR) in the folate pathway. MTX is considered as a crucial element in different ALL treatment protocols (4). DHFR produces THF, whereas Thymidylate Synthetase (TYMS) utilizes methylene-THF as its substrate. TYMS plays an important role in DNA synthesis and repair (5). TYMS contributes to antiproliferative properties by inhibiting the effect of methotrexate (6); thus, TYMS levels have been utilized to anticipate MTX therapeutic outcomes (7). Although methotrexate is very effective in the treatment of ALL, it has several disadvantages, some of which can be life-threatening (8, 9). The conventional approaches to administering chemotherapy as a pre-treatment for leukemia are associated with numerous limitations. Additionally, MTX resistance poses a significant obstacle to the success of ALL chemotherapy (8-10).

Carotenoids, being natural molecules, have undergone extensive research to explore their distinct characteristics in the treatment of different diseases (11). These lipophilic antioxidants exhibit diverse mechanisms of action, including electron transfer, hydrogen abstraction/reduction, and the creation of carotenoid-radical adducts (12). Consequently, they possess the ability to eliminate free oxygen radicals from the body, thereby aiding in the treatment of cancer and the prevention of tumor growth in individuals affected by this disease (13, 14).

Astaxanthin (AST), a common carotenoid, is found in the red pigments of shrimp, salmon, and crab. AST has demonstrated remarkable antioxidant, anti-inflammatory, and antitumor characteristics devoid of any significant negative effects (15-19).

Given the undeniable presence of side effects from chemotherapeutics and the emergence of drug resistance, it is imperative to develop new and potent medications that possess minimal toxicity. These novel treatments aim to enhance the response rate and ultimately prolong the overall survival of patients.

Due to the significant impact of oxidative stress on leukemia progression, we hypothesized that AST, with its established antioxidant and antitumor properties, could potentially mitigate the side effects of MTX. The study focused on evaluating the impact of AST, MTX, and their combination on oxidative stress, cell viability, cell cycle, and the expression of apoptotic, anti-apoptotic, and inflammatory genes in the NALM-6 pre-B ALL cell line.

## Materials and methods

### Cell culture

NALM-6 and HDF cell lines, were acquired from the Pasteur Institute of Iran. The cells were cultivated in Roswell Park Memorial Institute (RPMI) 1640 medium, which was obtained from Gibco in the United States. To support cell growth, the medium was supplemented with 10% de-



[ DOI: 10.22088/IJMCM.BUMS.13.2.133 ]

complemented Fetal Bovine Serum (FBS) also from Gibco, along with penicillin (100 U/mL) and streptomycin (100 µg/mL) from the same source. The cells were maintained at a temperature of 37 °C, with a humidity level of 95% and a CO2 concentration of 5%. The experiment was carried out during the exponential growth phase.

**Cell viability assay**

Nagoya Leukemia-Lymphoma Cell Line Number 6 (NALM-6) and Human dermal fibroblasts (HDF) cells were seeded at a density of $15\times10^3$ cells per well in triplicate in a 96-well microplate and exposed to varying concentrations of MTX (100-700 nM) (Ebewe, Austria) and AST (5-50 µM) (Sigma-Aldrich) for 24 hours. Cell viability was evaluated by the addition of 20 µL MTT solution (5 mg/mL, 100 µL/well) (Sigma–Aldrich) in each well. The formazan crystals were dissolved in 100 µL Dimethyl sulfoxide (DMSO) (Merck, Germany) after 4 hours of incubation at 37 °C. Finally, the absorbance was measured at 570 nm and 630 nm using Epoch microplate spectrophotometer (BioTek-Epoch, USA). The percentage of cell viability was calculated and compared to the control group.

**Co-treatment**

After determining the half-maximal inhibitory concentration (IC50) for each compound, the cells were subjected to treatment with different concentrations of MTX + AST. This was achieved by gradually decreasing the concentrations of MTX while maintaining the IC50 concentration of AST for a duration of 24 hours.

**Cell cycle arrest**

The progression of the cell cycle after treatment was evaluated using the flow cytometry technique. $1\times10^6$ cells/well were collected by centrifugation at 1200g for 5 minutes after 48h/24h treatment. These cells subsequently washed in phosphate buffered saline (PBS) twice. In each group, treated cells were first fixed in cold 70% ethanol and then resuspended in PBS after removing the ethanol. The fixed cells underwent two incubations: a 20-minute exposure to 0.3 µ RNase (Sina colon, Iran) (0.1 mg/mL) and Triton X-100 solution (0. 5%) at 37 °C, followed by a 30 minutes incubation with 50 µg/mL PI stain (Sigma-Aldrich, Germany) (50 µg/mL) at room temprature (RT) in the dark. The flow cytometry analysis of the cell cycle phase was performed using the FL2 channel of a flow cytometer (Sysmex XN2000, japan). Untreated cells were used as negative controls. A total of 10,000 cells were counted for each determination, and the data were analyzed by FlowJo software (Version 10).

**Colony formation assay**

To evaluate the growth potential of treated cells, their ability to generate colonies in a semi-solid medium was examined. The suspended cells ($6\times10^3$ cells/1.5 mL/well) for each treatment were seeded onto 6-well plates with 0.6% agar supplemented with RPMI and 10% FBS, which were then overlaid on a 1% agar gel. Subsequently, the cells were cultured at 37 °C in a 5% CO2 environment for a duration of 28 days. Following this incubation period, 200 µL of MTT solution (5 mg/mL) was introduced to each well and allowed to incubate for 24 hours. Images were captured



[ DOI: 10.22088/IJMCM.BUMS.13.2.133 ]

of colonies with over 50 cells were enumerated using Olympus microscope from Japan. Finally, the formula below was utilized to determine the colony formation efficiency (CFE) percentage.

$$CFE\% = \frac{\text{Number of colonies in the treated well}}{\text{Number of colonies in the untreated well}} * 100$$

**Quantitative reverse transcriptase-PCR**

The NALM-6 cells underwent treatment in four distinct groups, including AST, MTX, and AST+MTX, as treatment groups and the untreated cells as the control group in a 6-well plate for 24 hours. Following treatment, RNA extraction was carried out utilizing the Sinacolon extraction kit (Sinacolon, Iran), with subsequent reverse transcription performed using the Pars-Tous cDNA synthesis kit (Pars-Tous, Iran). RNA concentrations were determined using Nanodrop (Epoch, Biotek, USA), and RNA quality was analyzed by agarose gel electrophoresis (data not shown). The relative gene expression was measured by qRT-PCR method on the ABI 7300 cycler device (Applied Biosystems, USA). qRT- PCR by SYBR green PCR Master mix (Amplicon, Denmark) was performed under specific conditions. These conditions included 40 cycles consisting of 15 seconds at 95 °C for denaturation, 1 minute at 60 °C for annealing, and 30 seconds at 72 °C for extension. All PCR reactions were done in triplicate. Additionally, a melting curve analysis was carried out to evaluate the quality of the primers and products. The relative amounts of target genes were normalized with respect to GAPDH. To quantify transcripts, a comparative threshold cycle (CT) analysis was employed. The value was calculated using the $2^{-\Delta\Delta CT}$ method. The sequence of primers used for RT-PCR are as follows:

DHFR (forward, 5´- CCA CCG CTC AGG TAA ACA GA-3´; reverse, 5´- ATG GCC TGG GTG ATT CAT GG -3´), TYMS (forward, 5´- CCT CTG CTG ACA ACC AAA CG-3´; reverse, 5´- ATC ATG TAC GTG AGC AGG GC-3´). GAPDH (forward, 5´- AAG TTC AAC GGC ACA GTC AAG G-3´; reverse, 5´- CAT ACT CAG CAC CAG CAT CAC C-3´).

**FRAP assay (Ferric reducing antioxidant power)**

The FRAP method involves the conversion of the TPTZ (2, 4, 6-tri-yridyl--triazine)–Fe3+ compund to the TPTZ–Fe2+ compound with the addition of antioxidants and a strong color. The change in absorption is then measured. As a result, the yellow color of the sample transforms into various colors, depending on the antioxidant's reducing power. The fresh FRAP reagent (Kavosh Arian Azma, Iran) was heated to 37 °C for 30 minutes. Subsequently, 50µl of cell lysate from three different treated groups was added to 250µl of the FRAP reagent. After a 10-minute incubation period at room temperature, the measurement of absorbance was conducted. The values were determined using Trolox and the calibration curve.

**Statistical Analysis**

ANOVA was conducted to assess statistical significance between groups using GraphPad Prism software version 9.0 (La Jolla, California, USA). The normality of the data was evaluated through the Kolmogorov-Smirnov test. Statistical significance was determined at p-values of $\leq 0.05$. Each sample was replicated three times (n=3).



[ DOI: 10.22088/IJMCM.BUMS.13.2.133 ]

## Results

### Combined treatment of AST with low-dose MTX inhibited NALM-6 cell proliferation

First, the effects of different concentrations of AST and MTX on the growth and survival of NALM-6 were investigated. Following treatment, it was observed that low-dose MTX alone did not impede cell growth after different times of treatment, and cell viability as measured by MTT assay remained at approximately ~80% of the control from 24 to 48 h (Figure 1G). The IC50 dose of AST and MTX at 24h determined to be 25 µM and 300 nM, respectively. Notably, unlike MTX, the inhibition caused by AST was dose-dependent (Figure 1).

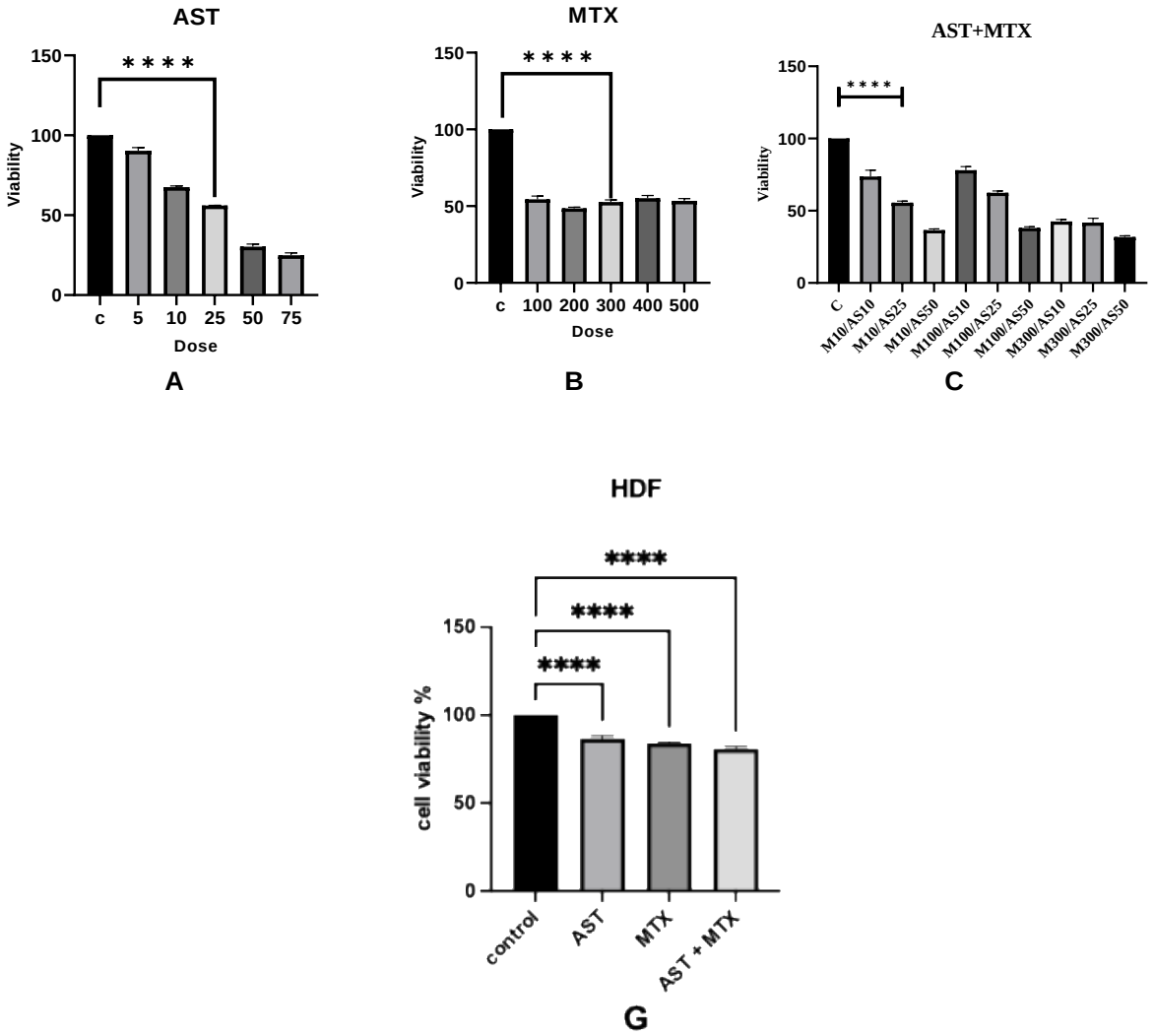


**Fig.1**. The effect of AST, MTX and AST+MTX on viability of NALM-6 cells by MTT assay. Cells were treated with different doses of AST, MTX and AST+MTX during a specific incubation period. The IC50 dose of AST and MTX was 25µM and 300nmol, respectively (A, B). The combination therapy of MTX and AST resulted in a substantial reduction in the necessary dosage of MTX to just one-thirtieth (10nmol). (C) There was also a notable decline in NALM-6 cell viability when compared to HDF cells. HDF cells treated with the IC50 value of different treatments which were used as the control group (G) (P<0.0001).



[ DOI: 10.22088/IJMCM.BUMS.13.2.133 ]

To identify the optimal combination doses of MTX with AST, different amounts of each were administered. Interestingly, an IC50 dose was achieved by the combination of 25 µM AST and 10 nM MTX. As depicted in Figure 1, the combined treatment involving low-dose MTX and the IC50 dose of AST effectively suppressed NALM-6 cell proliferation and survival. The investigation additionally assessed the cytotoxic effects of ATX and MTX on HDF, indicating that although the cell viability decreased, the rate of viability was considerably greater ($p < 0.0001$) compared to NALM-6 cells.

**Combined treatment of AST with low-dose MTX inhibited the colony formation ability**

The soft agar assay was employed to assess the colony formation capability of NALM-6 cells after a 24-hour treatment. The colony inhibition rates in AST, MTX, and AST+MTX groups were found to be 47%, 37% and 27%, respectively. All treated groups exhibited a significant decrease in the numbers of colonies when compared to the control group. These findings indicate that both AST and MTX individually limit the cloning ability of NALM-6 cells, but the combined treatment of AST+MTX demonstrates a superior effect (Figure 2).

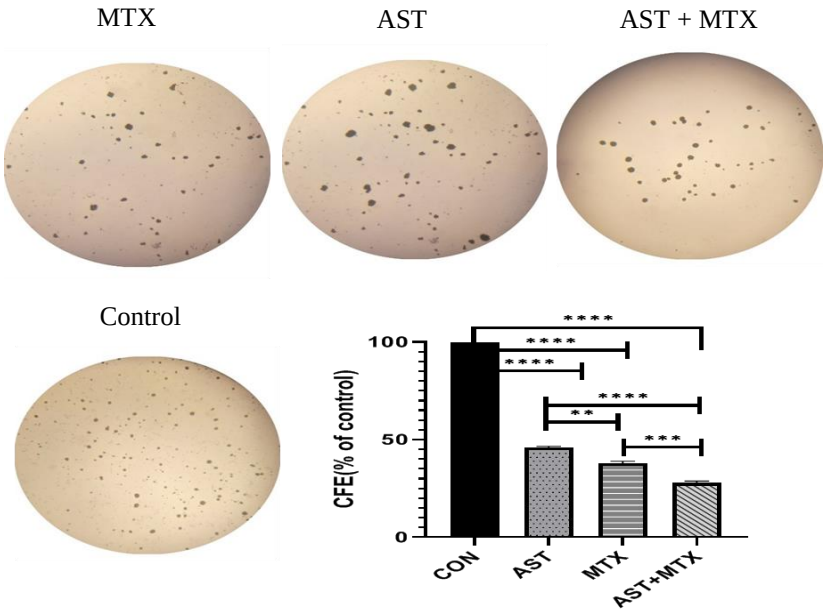


**Fig. 2**. Colony formation assay was performed by 24-h incubation of NALM-6 cells with AST (25 µmol), MTX (300nmol) and AST+MTX (25 µmol+10nmol) for 28 days. After the incubation, colonies were stained using MTT. The colony formation efficiency (CFE) was then calculated as a percentage of untreated cells (Control). The results showed the pronounced impact of AST+MTX in inhibiting the proliferation and colony formation of the NALM-6 cells (×40). (*** P< 0.001, ****, P < 0.0001).

**AST and MTX Induced Cell Cycle Arrest at G1 Phase in NALM-6 Cells**

Our study aimed to explore the potential relationship between the decrease in cell viability induced by AST and MTX and the arrest of the cell cycle. To achieve this, we utilized propidium iodide (PI) staining and flow cytometry to analyze the distribution of the cell cycle. Our findings revealed that the proportion of cells in the G1 phase increased in the treated group compared to the control group. Specifically, in NALM-6 cells, treatment with 25 µM AST, 300nM MTX, and a combination of 25 µM AST and 10 nM MTX



[ DOI: 10.22088/IJMCM.BUMS.13.2.133 ]

resulted in G1 phase distribution rates of 49.3%, 51.1%, and 61.7%, respectively, as opposed to the control rate of 45.4%. These results indicate that the combination of AST and MTX led to a more significant G1 arrest and G1/S ratio. Overall, our data suggest that AST, MTX, and their combination induced cell cycle arrest at the G1 phase in NALM-6 cells, potentially contributing to the observed reduction in cell viability following treatment (Figure 3).

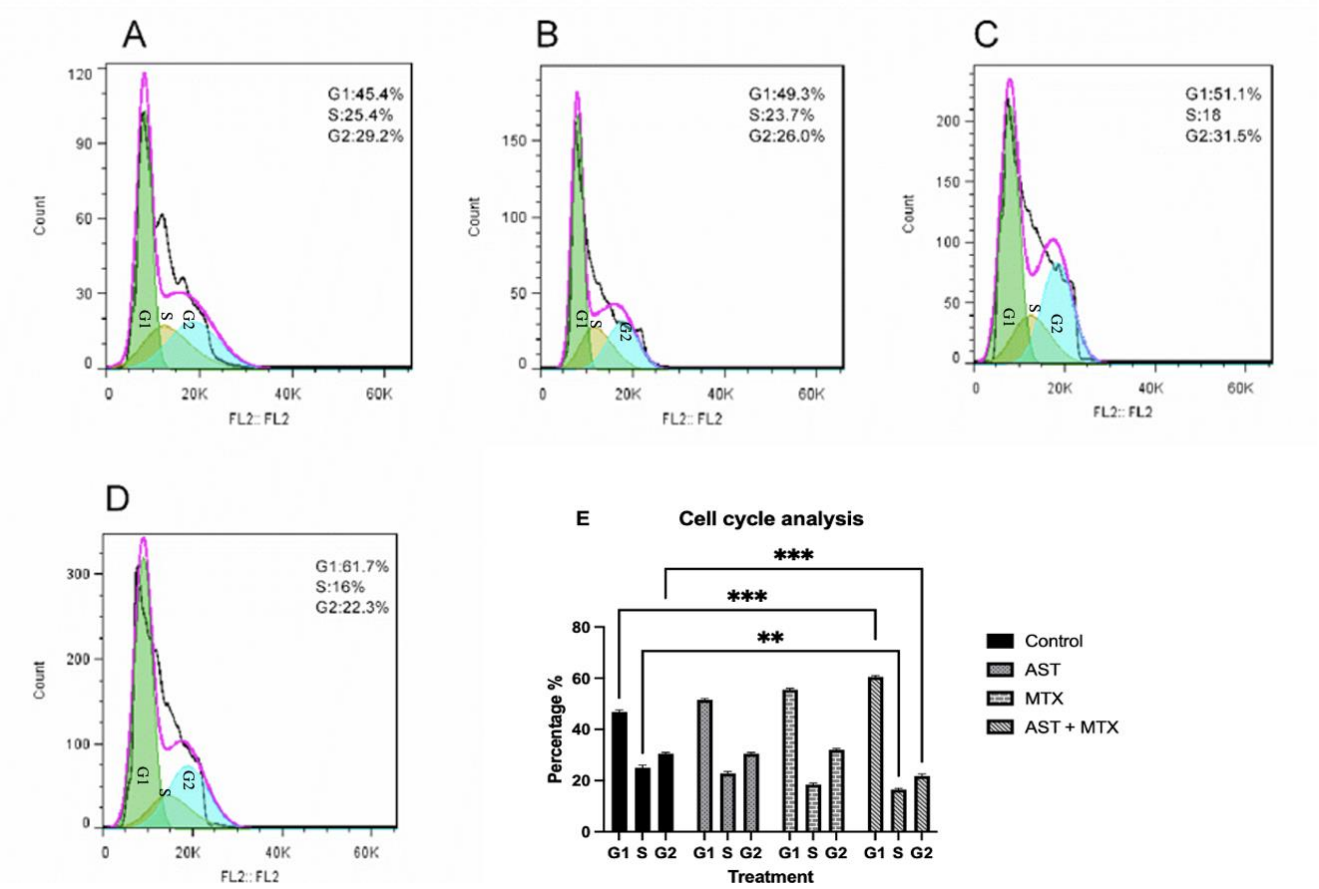


**Fig. 3**. Cell cycle analysis by flow-cytometry reveals that AST and MTX induced NALM-6 cell cycle arrest at the G1 phase. Control group without any treatment (A) NALM-6 cells treated with AST(B) MTX (C), and AST+MTX for 24 h (D). The cells were washed, fixed, and stained with PI and analyzed for DNA distribution by flow cytometry. Section (E) illustrates the percentages of NALM-6 cells in different phases of the cell cycle. As it is demonstrated AST+MTX combination can induce cell cycle arrest in G1 stage in NALM-6 cell line.

**The expression of TYMS and DHFR genes was down-regulated in treated cells**

To ensure the assessment of alterations in DHFR and TYMS expression levels, qRT-PCR was performed. As for the results, we detected that the DHFR and TYMS genes were down-regulated in all treated groups when compared to the untreated control cells ($p<0.0001$). Besides, the most remarkable result was obtained in the AST+MTX group, where the expression of DHFR was notably lower than in the other groups (Figure 4).





[ DOI: 10.22088/IJMCM.BUMS.13.2.133 ]

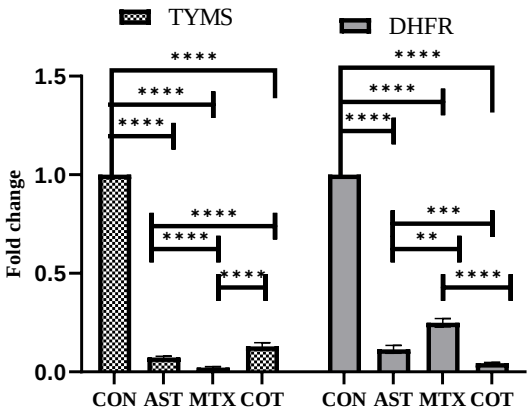


**Fig. 4**. Gene expression analysis by real-time PCR. Expression levels of TYMS and DHFR in control and NALM6 cells treated with AST, MTX, and AST+MTX after normalization against GAPDH were investigated. Data shows that DHFR and TYMS gene expression levels were significantly decreased in comparison to the untreated control cells (p<0.0001). ** P< 0.01, *** P< 0.001, ****, P < 0.0001.

**The expression of apoptotic genes was up-regulated in treated cells**

Results obtained from qRT-PCR indicated that all treatments exhibited an increase in the expression of Bcl-2-associated protein x (BAX) and caspase 3 (CASP3), while showing a decrease in the expression of the anti-apoptotic gene B-cell lymphoma-extralarge (Bcl-xL) in comparison to the control group (p-value<0.0001) (Figure 5).

**The expression of anti-apoptotic genes was down-regulated in treated cells**

Bcl-xL gene was 0.16, 0.20, and 0.205-fold down-regulated in AST, MTX, and AST+MTX treatment groups, respectively (p-value<0.0001) (Figure 5).

**AST, MTX, and AST+MTX up-regulated inflammation-related gene expression**

The effects of different treatments on inflammation were further investigated by analyzing the expression of TNFα and IL6 genes. Our results showed that administration of AST, MTX, and AST+MTX significantly rose the expression of both genes (p<0.0001). The TNFα expression was markedly reduced when AST+MTX were present, compared to the individual presence of AST or MTX alone (p<0.0001) (Fig5).

**STAT3 gene expression was down-regulated in treated cells**

Our results showed that AST+MTX> AST>MTX remarkably suppressed the mRNA expression of Signal Transducer and Activator of Transcription 3 (STAT3) (Figure 5).

## AST and AST+MTX increased antioxidant capacity

The FRAP assay results indicated the level of antioxidant capacity was significantly decreased by MTX in comparison to the control group (p-value <0.0001). Furthermore, this reduction was more pronounced in the AST and AST+MTX groups compared to the MTX group (p <0.0001). In other words, AST (25µM) and AST+MTX (25µM+10nM) treatments resulted in a maximum reduction of iron ion by 114 and 117 equivalent Trolox, respectively, while MTX (300nM) exhibited 74 equivalent Trolox. The control group had an equivalent Trolox value of 137(Figure 6).



[ DOI: 10.22088/IJMCM.BUMS.13.2.133 ]

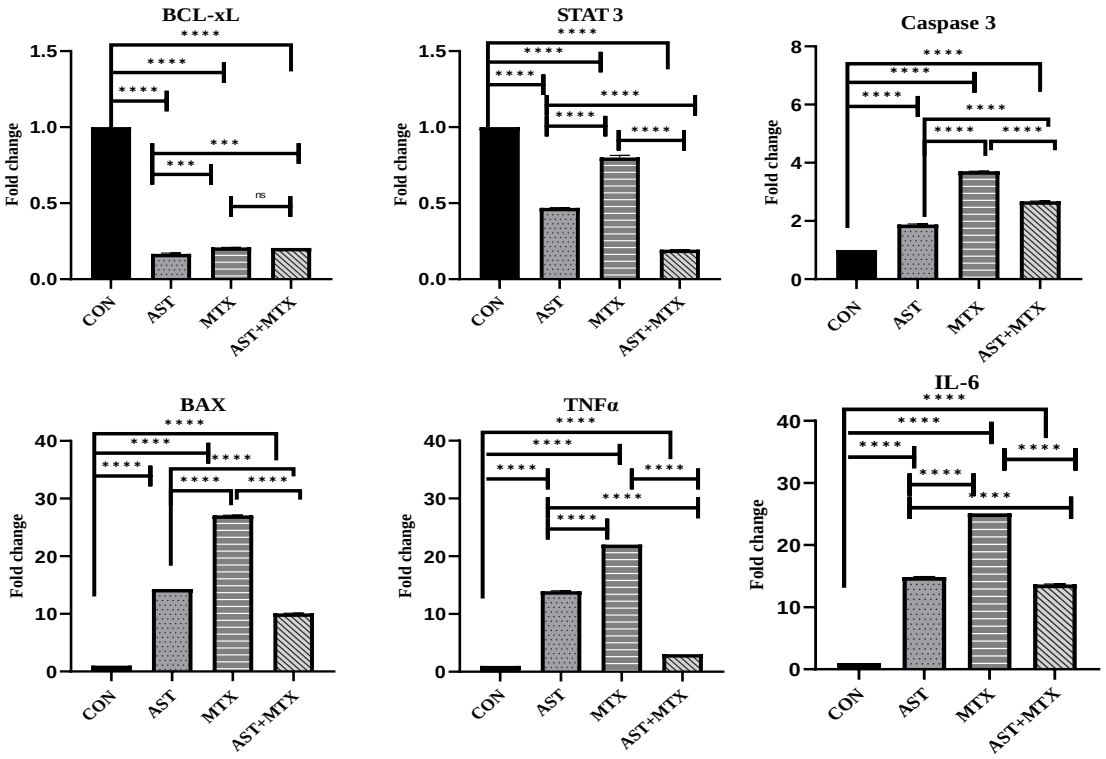


**Fig. 5**. Evaluation of Gene expression by real-time PCR The expression level of apoptotic, anti-apoptotic and inflammatory genes in treated groups and untreated control cells. In the treated cells, the expressions of CASP3 and BAX were found to be higher than in the control cells. The BCL-2, an anti-apoptotic gene, and STAT3 showed decreased expression levels. An increase was also observed in the expression of TNF-α and IL-6 in treated groups compared to the control group.

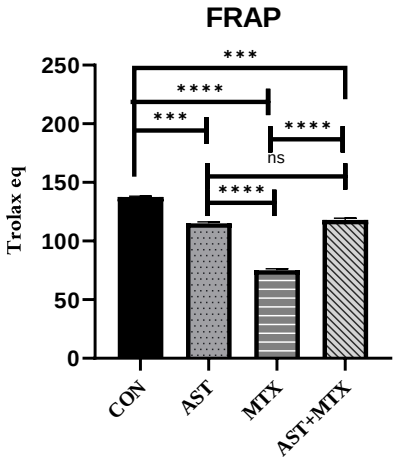


**Fig. 6**. The $Fe^{3+}$-$Fe^{2+}$ reducing activity of AST, MTX, and AST+ MTX based on FRAP assay. Data is represented as means±SD from three experiments, each experiment performed in triplicate. Data reveals that AST both in combination with MTX or alone can increase NALM-6 cell line antioxidant capacity. (****p < 0.0001, ***p 0.001, ns: non-significant).



[ DOI: 10.22088/IJMCM.BUMS.13.2.133 ]

## Discussion

Methotrexate, an antifolate medication, primarily focuses on DHFR and TYMS genes. Given the numerous adverse effects linked to MTX as a cancer treatment, there is a pressing requirement to explore substitute substances that can lower the dosage of this medication while maintaining its anti-cancer characteristics (20).

Astaxanthin, a carotenoid xanthophyll with a red-orange hue, is recognized for its diverse clinical and pharmacological advantages, including its anti-cancer, antioxidant, and anti-inflammatory characteristics (17).

As far as our understanding goes, there has been no previous investigation conducted to examine the influence of AST on MTX-induced toxicity in the NALM-6 cell line. Consequently, the aim of this present study was to evaluate whether co-administration of AST could mitigate the dosage of MTX, enhance its cytotoxicity effects, or alleviate the MTX-induced inflammatory response.

Our research showed the significant suppressive impact of AST on the survival of NALM-6 cells. Moreover, the survival rate of HDF cells showed a marked increase compared to NALM-6 cells, with statistical significance ($p< 0.0001$). Likewise, Ganesanet al. revealed similar outcomes against human leukemia (HL-60) cell line (11). The interesting result of the current study was that the administration of AST (25µM) effectively reduced the MTX dosage by one-thirty (10 nM) to reach the IC50 in the NALM-6 cell line. This may be due to the fact that AST could inactivate PI3K/AKT signaling pathway. Subsequently, a decline in Bcl-2 expression and an elevation in Bax levels occur, culminating in the initiation of apoptosis. (17). Given that lower doses have the potential to mitigate the adverse effects associated with the medication, this amalgamation appears to hold significant value.

In the present investigation, the combination of AST and MTX resulted in a significantly higher G1 arrest compared to AST and MTX alone, despite both AST and MTX individually increasing cell cycle arrest in the G1 phase. Xia Zhang et al. conducted a study on the effect of carotenoids on peroxisome proliferator-activated gamma receptor (PPARγ) and demonstrated that AST could inhibit proliferation and reduce survival of K562 cells in a dose- and time-dependent manner through apoptosis and disruption of cell cycle progression (14). It has shown that AST in K562 causes p21 activation and cyclin D1 inhibition, leading to cell cycle arrest at the G0/G1 phase (21). In our prior investigation, we have shown that the combination of AST therapy and imatinib can effectively reduce the viability of cells in the K562 cell line in a dose-dependent manner. In this study, we have additionally explored the beneficial anti-leukemic properties of crocin, a natural carotenoid. Our findings unequivocally demonstrate that the utilization of these two dietary carotenoids can significantly lower the required dosage of imatinib to achieve IC50 levels. Furthermore, this combination induces cell cycle arrest in the G1 phase and enhances the expression of apoptosis genes, while simultaneously suppressing the expression of anti-apoptotic and inflammatory genes (22).

An increase in cells in the G1 phase and a decrease in S and G2/M phases were observed when treating the HL-60 leukemia cell line with AST (23). Colon cancer cells treated with astaxanthin-rich alga Haematococcus Pluvial exhibited a dose-dependent reduction in cyclin D4 and p-ERK and a dose-dependent increase in p27Kip-1, p21WAF-1/CIP1, and p53. (24, 25). Cyclin D, the first cyclin formed in the cell cycle,



[ DOI: 10.22088/IJMCM.BUMS.13.2.133 ]

becomes activated when it binds to cyclin-dependent kinase 4 (CDK4). This complex then phosphorylates Rb causing p-Rb to separate from the E2F/DP1/Rb complex. E2F activation leads to cyclin E transcription and binding to CDK2, which finally drives cells from G1 to S phase (24). On the other hand, downregulation of the p-ERK inhibits the cyclin D1/CDK4 complex. Besides, augmented level of p27Kip-1 is associated with the suppression of cyclin E/CDK2 complex. These processes contribute to cell cycle arrest at the G0/G1 phase (24, 26).

Colony formation assay ultimately demonstrated that AST not only inhibits cell proliferation but also synergistically enhances the inhibitory effect of MTX on cell colony formation ability in NALM-6 cells. We examined TYMS and DHFR expression in NALM-6 cells. Treatment of the cells with AST for 24 h, MTX for 48 h, and AST+MTX resulted in a decrease in the expression of both genes. It has been argued that expression of DHFR and TYMS is connected to DNA synthesis and cell proliferation. MTX is known to target cells in the S-phase of the cell cycle by irreversibly binding to DHFR, resulting in the diminution of tetrahydrofolate intracellular reservoir and reduced DNA synthesis (27). DHFR and TYMS are also affected by other factors such as miR-192 whose decreased expression is associated with higher levels of these genes in MTX resistance in ALL patients (28).

Zhewei Fei et al., discovered that knocking down of DHFR by siRNA leads to cell cycle arrest in the G1 phase (29). Additional reports from Meng et al. (30) and Lee et al. (31) showed that DHFR overexpression in certain cancer cell lines is a known mechanism of resistance to chemotherapy using MTX. These studies collectively highlight the significance of inhibiting DHFR and TYMS in the treatment of ALL patients and in preventing methotrexate resistance.

We evaluated the effect of AST, MTX, and AST+MTX on the expression levels of Bax and CASP3, which are known to promote apoptosis (Fig. 5D), as well as Bcl-XL, a suppressor of programmed cell death in NALM-6 cells. All treatments resulted in a significant increase in Bax and CASP3 expression, while reducing Bcl-XL expression compared to the control group ($P < 0.05$). Caspase-3, a crucial protease involved in activation of both the extrinsic and intrinsic apoptosis pathways, serves as a key indicator of the irreversible stage of apoptosis.

Interestingly, the expression of Bax and CASP3 was diminished in the presence of AST compared to the MTX group. This suggests that AST may act as a protective agent against MTX toxicity by inhibiting excessive apoptosis and its activity reducing properties. These findings are consistent with a study by Yuksel et al., where they observed that MTX increased CASP3 expression, which was then reduced by co-treatment with the antioxidant Quercetin (32). Similarly, Hormozi et al. found that AST induces apoptosis and inhibits proliferation and growth by upregulating the expression of Bax and Caspase3 genes while downregulating the expression of Bcl2 in LS-180 cells (33).

In all treatment groups, a decreased in STAT3 expression was observed; however, the effect of AST and particularly AST+MTX was remarkably greater than that of MTX alone. Among the STAT protein family, the persistent activation of STAT3 is commonly observed in cancer cells, playing a major role in the apoptosis pathway (17). Kowshik et al. found that AST disrupted STAT3 phosphorylation and its subsequent nuclear translocation, leading to the downregulation of target genes associated with cyclin D1 proliferation (34).



[ DOI: 10.22088/IJMCM.BUMS.13.2.133 ]

AST has been found to trigger mitochondrial apoptosis in rat hepatocellular carcinoma cells by inhibiting the JAK/STAT3 signaling pathway (35). In the context of rat hepatocellular carcinoma cells, a thorough investigation was carried out by Song et al. Their study uncovered the significant contribution of AST in triggering apoptosis in these cells. This was achieved by suppressing the expression of STAT3 and its upstream activator, JAK1.Consequently, this interference disrupts the normal regulation of gene expression associated with the anti-apoptotic targets of STAT3 (36). Nevertheless, the absence of protein analysis data posed a constraint on our research.

Our results also showed that methotrexate had an impact on the expression of inflammatory genes, specifically IL-6 and TNF-α compared to the control group. However, when AST and AST+MTX were examined, we found that the expression of both genes decreased. Li et al. reported that AST considerably decreased the production of TNF-α and IL-17 in lipopolysaccharide stimulated neutrophils. They proposed that this effect was due to the suppression of NF-kB activation, which is a key transcription factor for inducible nitric oxide synthase .This suppression may be attributed to the scavenging of intracellular Reactive oxygen species (ROS). As a result, the production of these inflammatory cytokines was efficiently inhibited (17, 37- 38). Moreover, NF-kB regulated the expression of proteins related to proliferation (cyclin D1) and apoptosis (Bcl-2, Bcl-xL) (17).

FRAP assay was performed to assess the ability of AST to scavenge free radicals in a laboratory setting (in-vitro) (expressed as equivalent Trolox value) through utilizing its iron reducing capacity. It has been demonstrated that the FRAP method is highly sensitive in quantification of total antioxidant capacity of pharmacological products (38). The obtained results in our study indicated that AST possesses a strong iron-reducing ability, effectively counteracting the oxidant effect of MTX on NALM-6 cells. In U937 cells, AST has been shown to attenuate intracellular $O2^-$ production by restoring the antioxidant function of superoxide dismutase and catalase, consequently reversing ROS production and lipopolysaccharide-induced toxicity (39). Accordingly, oxidative stress is likely a significant factor connecting AST to cell proliferation and apoptotic commitment (17).

The findings from multiple tests conducted in our research revealed, for the first time the involvement of AST in restraining leukemic cell proliferation, regulating cell cycle transition, and inhibiting colony formation of the NALM-6 cells. Moreover, AST demonstrated the potential to mitigate the dosage of MTX and alleviate the side effects associated with chemotherapy. These results position AST as a promising candidate for chemotherapeutic treatment. To gain a deeper comprehension of AST's impact on ALL, additional in vitro and in vivo investigations should be carried out.

**Acknowledgments**

The Institutional Ethics Committee at BUMS, Iran (IR.BUMS.REC.1399.551) granted approval for the comprehensive protocol utilized in this study. Our gratitude extends to BUMS for their invaluable support and provision of laboratory resources. The financial support for this research was provided by Birjand University of Medical Sciences, Birjand, Iran (Grant number: 5607).

## References

1. Puntis D, Malik S, Saravanan V, et al. Urinary tract infections in patients with rheumatoid arthritis. Clin Rheumatol 2013;32: 355-60.



[ DOI: 10.22088/IJMCM.BUMS.13.2.133 ]

2. Paul S, Kantarjian H, Jabbour EJ. Adult Acute Lymphoblastic Leukemia. Mayo Clin Proc 2016;91:1645-66.

3. Sakura T, Hayakawa F, Sugiura I, et al. High-dose methotrexate therapy significantly improved survival of adult acute lymphoblastic leukemia: a phase III study by JALSG. Leukemia 2018;32:626-32.

4. Gong F, Meng Q, Liu C, et al. Efficacy and association analysis of high-dose methotrexate in the treatment of children with acute lymphoblastic leukemia. Oncol Lett 2019;17:4423-8.

5. Antosiewicz A, Jarmula A, Przybylska D, et al. Human dihydrofolate reductase and thymidylate synthase form a complex in vitro and co-localize in normal and cancer cells. J Biomol Struct Dyn 2017;35:1474-90.

6. Rushworth D, Mathews A, Alpert A, et al. Dihydrofolate Reductase and Thymidylate Synthase Transgenes Resistant to Methotrexate Interact to Permit Novel Transgene Regulation. J Biol Chem 2015;290:22970-6.

7. Oosterom N, Berrevoets M, den Hoed MAH, et al. The role of genetic polymorphisms in the thymidylate synthase (TYMS) gene in methotrexate-induced oral mucositis in children with acute lymphoblastic leukemia. Pharmacogenet Genomics 2018;28:223-9.

8. Haso W, Lee DW, Shah NN, et al. Anti-CD22-chimeric antigen receptors targeting B-cell precursor acute lymphoblastic leukemia. Blood 2013;121:1165-74.

9. Sajith M, Pawar A, Bafna V, et al. Serum Methotrexate Level and Side Effects of High Dose Methotrexate Infusion in Pediatric Patients with Acute Lymphoblastic Leukaemia (ALL). Indian J Hematol Blood Transfus 2020;36:51-8.

10. Wojtuszkiewicz A, Peters GJ, van Woerden NL, et al. Methotrexate resistance in relation to treatment outcome in childhood acute lymphoblastic leukemia. J Hematol Oncol 2015;8:61.

11. Yu L, Wang L, Chen S. Endogenous toll-like receptor ligands and their biological significance. J Cell Mol Med 2010;14: 2592-603.

12. Perez-Galvez A, Viera I, Roca M. Carotenoids and Chlorophylls as Antioxidants. Antioxidants (Basel) 2020;9.

13. Bhatt T, Patel K. Carotenoids: Potent to Prevent Diseases Review. Nat Prod Bioprospect 2020;10:109-17.

14. Bedhiafi T, Inchakalody VP, Fernandes Q, et al. The potential role of vitamin C in empowering cancer immunotherapy. Biomed Pharmacother 2022;146:112553.

15. Ekpe L, Inaku K, Ekpe V. Antioxidant effects of astaxanthin in various diseases—A review. J Mol Pathophysiol 2018;7:1-6.

16. Fakhri S, Abbaszadeh F, Dargahi L, et al. Astaxanthin: A mechanistic review on its biological activities and health benefits. Pharmacol Res 2018;136:1-20.

17. Zhang L, Wang H. Multiple Mechanisms of Anti-Cancer Effects Exerted by Astaxanthin. Mar Drugs 2015;13:4310-30.

18. Kheyrandish S, Rastgar A, Hamidi M, et al. Evaluation of anti-tumor effect of the exopolysaccharide from new cold-adapted yeast, Rhodotorula mucilaginosa sp. GUMS16 on chronic myeloid leukemia K562 cell line. Int J Biol Macromol 2022;206:21-8.

19. Rastgar A, Sayadi M, Anani-Sarab G, et al. Astaxanthin decreases the growth-inhibitory dose of cytarabine and inflammatory response in the acute lymphoblastic leukemia cell line NALM-6. Mol Biol Rep 2022;49:6415-22.

20. Garcia-Canaveras JC, Lancho O, Ducker GS, et al. SHMT inhibition is effective and synergizes with methotrexate in T-cell acute lymphoblastic leukemia. Leukemia 2021;35:377-88.

21. Zhao H, Gu H, Zhang H, et al. PPARgamma-dependent pathway in the growth-inhibitory effects of K562 cells by carotenoids in combination with rosiglitazone. Biochim Biophys Acta 2014;1840:545-55.

22. Golestani A, Rahimi A, Najafzadeh M, et al. "Combination treatments of imatinib with astaxanthin and crocin efficiently ameliorate antioxidant status, inflammation and cell death progression in imatinib-resistant chronic myeloid leukemia cells". Mol Biol Rep 2024;51:108.



[ DOI: 10.22088/IJMCM.BUMS.13.2.133 ]

23. Bechelli J, Coppage M, Rosell K, et al. Cytotoxicity of algae extracts on normal and malignant cells. Leuk Res Treatment 2011;2011:373519.

24. Kim HY, Kim YM, Hong S. Astaxanthin suppresses the metastasis of colon cancer by inhibiting the MYC-mediated downregulation of microRNA-29a-3p and microRNA-200a. Sci Rep 2019;9:9457.

25. Liu X, Song M, Gao Z, et al. Stereoisomers of Astaxanthin Inhibit Human Colon Cancer Cell Growth by Inducing G2/M Cell Cycle Arrest and Apoptosis. J Agric Food Chem 2016;64:7750-9.

26. Dong W, Zhu H, Gao H, et al. Expression of Cyclin E/Cdk2/p27(Kip1) in Growth Hormone Adenomas. World Neurosurg 2019;121:e45-e53.

27. Kawami M, Honda N, Hara T, et al. Investigation on inhibitory effect of folic acid on methotrexate-induced epithelial-mesenchymal transition focusing on dihydrofolate reductase. Drug Metab Pharmacokinet 2019;34:396-9.

28. Sayadi M, Rostami S, Nadali F, et al. miR-192 overexpression effect on DHFR and TYMS in acute lymphoblastic leukemia. Gene Rep 2020;21:100887.

29. Fei Z, Gao Y, Qiu M, et al. Down-regulation of dihydrofolate reductase inhibits the growth of endothelial EA.hy926 cell through induction of G1 cell cycle arrest via up-regulating p53 and p21(waf1/cip1) expression. J Clin Biochem Nutr 2016;58:105-13.

30. Meng XN, Ma JF, Liu YH, et al. Dynamic genomic changes in methotrexate-resistant human cancer cell lines beyond DHFR amplification suggest potential new targets for preventing drug resistance. Br J Cancer 2024;130:1819-27.

31. Lee YH, Yang HW, Yang LC, et al. DHFR and MDR1 upregulation is associated with chemoresistance in osteosarcoma stem-like cells. Oncol Lett 2017;14:171-9.

32. Yuksel Y, Yuksel R, Yagmurca M, et al. Effects of quercetin on methotrexate-induced nephrotoxicity in rats. Hum Exp Toxicol 2017;36:51-61.

33. Hormozi M, Ghoreishi S, Baharvand P. Astaxanthin induces apoptosis and increases activity of antioxidant enzymes in LS-180 cells. Artif Cells Nanomed Biotechnol 2019;47:891-5.

34. Kowshik J, Baba AB, Giri H, et al. Astaxanthin inhibits JAK/STAT-3 signaling to abrogate cell proliferation, invasion and angiogenesis in a hamster model of oral cancer. PLoS One 2014;9:e109114.

35. Li J, Dai W, Xia Y, et al. Astaxanthin Inhibits Proliferation and Induces Apoptosis of Human Hepatocellular Carcinoma Cells via Inhibition of Nf-Kappab P65 and Wnt/Beta-Catenin in Vitro. Mar Drugs 2015;13:6064-81.

36. Song X, Wang M, Zhang L, et al. Changes in cell ultrastructure and inhibition of JAK1/STAT3 signaling pathway in CBRH-7919 cells with astaxanthin. Toxicol Mech Methods 2012;22:679-86.

37. Li MY, Sun L, Niu XT, et al. Astaxanthin protects lipopolysaccharide-induced inflammatory response in Channa argus through inhibiting NF-kappaB and MAPKs signaling pathways. Fish Shellfish Immunol 2019;86:280-6.

38. Raja R, Hemaiswarya S, Arunkumar K, et al. Antioxidant activity and lipid profile of three seaweeds of Faro, Portugal. Rev Bras Bot 2016;39:9-17.

39. Franceschelli S, Pesce M, Ferrone A, et al. Astaxanthin treatment confers protection against oxidative stress in U937 cells stimulated with lipopolysaccharide reducing O2- production. PLoS One 2014;9:e88359.



[ DOI: 10.22088/IJMCM.BUMS.13.2.133 ]